Vol. 2(1), pp. 1-14, 2023
eISSN: 2976-4009

ASEAN Journal of Process Control

Research Article

Dynamic Simulation and Optimization of Chemical Looping Hydrogen Production in Inter-Connected Moving Bed Reactors

Priyam Kataria, Jobrun Nandong*, Wan Sieng Yeo

Departmentof Chemical and Energy Engineering, Faculty of Engineering and Science, Curtin University Malaysia, CDT 250, 98009 Miri, Sarawak, MALAYSIA

*Corresponding Author: jobrun.n@curtin.edu.my

Academic Editor: Syamsul Rizal Abd Shukor

Received: 7 December 2023; Accepted: 14 December 2023; Published: 31 December 2023

Abstract: The current study investigates the dynamics of the chemical looping hydrogen production (CLHP) process, which consists of three interconnected moving-bed reactors (MBRs) that circulate a solid oxygen carrier (OC). The OC undergoes redox reactions in each unit to generate various product gases, including the target hydrogen (H_2) gas, which is a highly efficient fuel source. The first two reactors known as the reducer and oxidizer respectively, were simulated in the MATLAB environment. The reactions are assumed to be conducted within a multi-tubular vessel while the pellet-grain model (PGM) was employed to represent the gas-solid interaction within a single particle, due to its reliability proven through several studies. The initial test data for reducer was retrieved from previous investigations, involving experimental verification and evaluation of the flow rates. Solid achieved the target phase for the oxidizer process, though a significant amount of unconverted gas (~ 27.5 %) was present in the outlet stream due to flow restrictions. The analysis was extended in this study by testing under reduced pellet sizes, where impurity concentrations as low as 6.5 mol% were achieved. The system was further investigated by varying the reaction temperature, which exhibited sufficient conversions (> 95%) for implementing a carbon capture strategy. A critical trade-off point was observed at 1070 K, which can be utilized for developing a temperature control system within the reactor. The oxidizer was simulated using reducer output flows to represent inter-connectivity, aimed at describing continuous production characteristics. Co-current and counter-current flows were compared for the reactor design, where the former regime was considered suitable due to a larger effective reaction zone. Due to several restrictions from the reducer, the process within the oxidizer could only be tested under the effect of reaction temperature. The optimum H_2 concentration (~ 34 mol%) recorded at 950 K, which must be controlled within a narrow range (± 5K) to ensure consistent quality. These findings indicated the importance of maintaining isothermal operation, which could be potentially solved through an effective tubular reactor design. The third unit called combustor was not included due to unavailability of the reaction kinetics, serving as prospects for further research in the field. Control system and scale-up design implications of the two reactors were further discussed, serving as essential information for future investigations. The findings presented within this study are vital contributions to the presently available research on CLHP, which is an important process for producing affordable green hydrogen fuel.

Keywords: Chemical looping hydrogen production, dynamic model, isothermal, optimization, inter-connected reactor system

1. Introduction

Energy is a consistent pursuit of every individual, given its necessity to sustain and improve the quality of life. Other than the fundamental requirements, fuel and electricity serve as key sources for various day-to-day operations. The sharp population growth since the industrial revolution has resulted in a considerable global demand [1]. The heavy reliance on modern technology and recent advancements further add to the elevated consumption, as evident by the three-fold increase within the energy usage per capita (per individual) in Malaysia over a three-decade period between 1984 – 2014 [2]. Although several alternatives have been implemented over the recent decades, the statistics indicate a significant rise in the fossil fuel-based applications over the same period (87% in 1984 and 97% in 2014) [3]. The percentage of alternative energy sources have also reduced (11% in 1984 and 1.3% in 2014), indicating that the supply is incapable of coping with the current demand [4].

A major issue arising from the non-renewable resources is through emission of greenhouse gases (GHGs) such as carbon dioxide (CO_2), leading to negative environmental impact through global warming [5]. In Malaysia, non-replenishable fuels such as coal, crude oil and natural gas, contributed around 93.3% of the total CO_2 emissions in 2020 (239 out 256 million tons total) [6]. The limited availability of fossil fuels presents another critical issue, which may lead to an energy crisis in the future. Thus, the current barriers to the energy industry require research towards sustainable alternatives, which can reduce emissions while simultaneously satisfying the increasing global demand. . Solar, wind, and geothermal technologies rely particularly on the weather, and require expensive battery storage to achieve continuous production [7]. Biomass-derived synthesis gas (Bio-syngas) is another possibility due to abundant availability, although the low yield and thermal efficiency necessitate implementation at a massive scale [8]. Nuclear fuels can generate an enormous amount of power at smaller scales, though the safety and disposal issues are critical elements preventing their commercialization [9, 10].

Hydrogen (H_2) is an excellent alternative due to its energy efficiency in fuel cells, along with clean combustion products (Steam or H_2O) [11]. Recent studies have also highlighted the possibility of producing H_2 through biomasses from various industries, which contributes to net-zero carbon emissions and co-integration potential [12, 13]. Literatures further demonstrate pathways for incorporating carbon capture and storage (CCS) systems, along with additional commercial applications for the produced CO_2 gas [14, 15]. Steam methane reforming (SMR) is a significant production process, which currently generates majority of the global H_2 supply. The SMR system reforms the natural gas fuel (primarily methane or CH_4) into a syngas product (CO and H_2 gas), which is further converted to CO2 and H_2 mixture through catalytic shift reactions. The produced gas fuels are separated using the pressure swing adsorption (PSA) unit to achieve a high-purity (< 99.9%) product. Despite outperforming several H_2 production processes, the economic efficiency of SMR is considerably lower than typical fossil-fuel based plants [16, 17]. Combustion within the reformer requires high energy demand to achieve adequate temperatures, which can incur considerable utility expenses. Moreover, the PSA equipment represent a significant cost within the process due to extensive capital and operating demand. Addition of a PSA unit for CCS can increase production costs by two to three times in comparison to the standard operation [18, 19]. These inefficiencies are reflected through the prices of H_2-based electricity (0.05-0.07$/kWh), representing a two to three times higher cost than coal/gas-fired industries [20, 21]. Operating expenditures are consistent throughout plant lifetime and exhibit a critical barrier towards widespread acceptance of H_2 as a fuel source. Developed economies are adopting the current SMR-based H_2 as a clean energy initiative, though the issue of affordability persists within developing nations and fossil fuels continue to dominate the supply [22-25].

Chemical looping combustion (CLC) is a well-known technology since the early 20th century, with several published patents between 1950 – 1980 [26-28]. The CLC process utilizes a metallic oxygen carrier (OC) to undergo redox cycles, while interacting with gases to form products. Early concepts were limited by the capability of gas-solid reactors for continuous solid circulation (Fixed-bed), which prevented the process from achieving mass industrial application. Moving-bed reactor (MBR) represents a significant feat of chemical and mechanical engineering which has restored research interest towards vital gas-solid processes such as CLC [29]. Chemical looping hydrogen production (CLHP) is a three-reactor CLC

concept, which can provide effective purification of the product gases without the PSA system. Additional/ advantages include the possibility of utilizing affordable solid OCs such as iron, as opposed to nickel for the SMR process [30]. Experimental investigations of CLHP using bench-scale equipment have produced promising results, demonstrating the capability to generate high-purity H_2 and effective CCS application [31]. The key issue surrounding this technology is the lack of dynamic process models, primarily due to the complexity of gas-solid interactions. The intricacy of reaction kinetics presents a challenging task to develop mathematical models representing the entire system. Limited number of studies have attempted to formulate dynamic process models for CLHP, primarily restricted to the analysis of a single reactor unit [32, 33]. Some investigations have also verified the findings from literature, thus confirming the validity of the proposed model [34]. Although the individual reactor simulation is necessary for model verification, it may not be adequate for process optimization. This is due to the inherent connectivity of MBRs within the closed-loop configuration, which may impose additional constraints during production. Few recent literatures have modelled the connected system through software such as ASPEN, however the simulation could only evaluate the process under steady-state operation [35]. Detailed mathematical models can determine the unsteady characteristics of the process, which are necessary for commercial reactor design. Such systems can also be used for testing control applications and identify key issues which preventing the system from achieving optimum operation. However, no known research has formulated the dynamic system of co-integrated reactors. The current study attempts to bridge this crucial research gap by demonstrating the unsteady dynamics of the first two CLHP reactors, developed within the MATLAB (r2020a) framework. The MBR units are assumed to operate under controlled temperatures (isothermal), which is possible through the implementation of multi-tubular configuration [36-38]. The system is tested through modification of essential parameters along with potential constraints, to optimize the product conversions. The third reactor is not included as part of simulation due to unavailability of the reaction kinetics for the process, serving as an essential prospect for further research. Nevertheless, this study represents a vital extension to the existing literature and provided vital information regarding the commercial implications of the CLHP technology.

2. Materials and Methods

The CLHP system comprises of an OC circulating among three reactors, where each reaction is targeted towards a specific oxidation state. Kang, Kim [39] conducted a comprehensive review of the reactant solids capable of being utilized within chemical looping applications. Iron-based OCs were identified superior for large-scale implementation, due to their lower prices, widespread commercial availability, and relatively high redox performance.

2.1. Chemical looping hydrogen production

A schematic illustration of the CLHP process can be referred from Figure 1, highlighting the reactant and product states at each stage. The first unit is known as the reducer, which converts the initial hematite (Fe_2O_3) state to a wüstite/iron (FeO/Fe) mixture. Bio-syngas represents a potential solution for achieving green H_2 production and is thus preferred for meeting the sustainability criteria. The oxidized gas within the reducer is a mixture of CO_2 and steam (gasified H_2O), which can be readily purified through condensers. This strategy demonstrates a crucial benefit of employing the CLHP process, as it can avoid the expenses incurred by PSA units.

The second reactor called oxidizer utilizes high-pressure steam to partially oxidize the solid into magnetite (Fe_3O_4) state. The gas mixture is reduced to H_2/H_2O state, and pure product can be retrieved through a condenser identical to the CSS (for reducer). The condensed steam from both reducer and oxidizer can recovered and re-pressurized for effective recycling, exhibiting an additional economic advantage. The Fe_3O_4 OC further advances to the combustor, where contact with high-temperature air oxidizes the solid, consequently restoring the initial Fe_2O_3 state. This reactor is vital for achieving continuous production as the oxidizer process is thermodynamically limited [40]. The combustion with air is a highly exothermic process, which provides heat recovery pathways for satisfying demand [41].

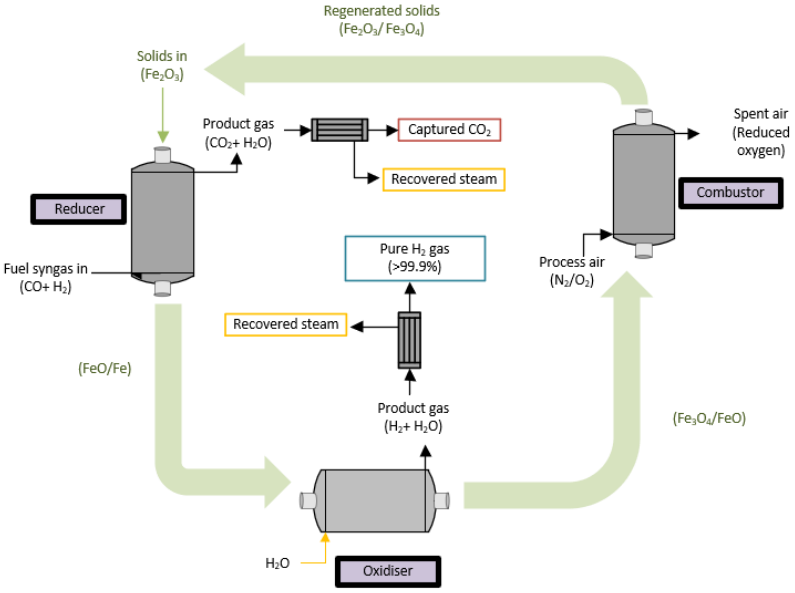

Figure 1. The three-reactor CLHP process [40]

2.2. Dynamic modelling procedures

The proposed simulation is developed within the MATLAB r2020a framework, utilizing multiple codes (m-files) compiled into a Simulink model. The process kinetics are formulated through the pellet-grain model (PGM), where the gas species diffuse into a porous pellet to undergo reactions [42]. PGM represents an extension of the well-known shrinking core model (SCM), comprising additional computations accounting for changes in pellet porosity. This mathematical procedure has been implemented within literature to study the kinetics of various industrial gas-solid processes, along with a comparison against experimental profiles for verifying accuracy [43-45]. Rahimi and Niksiar [34] investigated the application of PGM for demonstrating reduction of spherical Fe_2O_3 pellets through syngas, facilitated within a MBR environment. The system was tested at multiple operating conditions for verifying the metrics against the experimental work conducted by Takenaka, Kimura [46]. The results produced an average error of around 1.2 %, which suggests the validity of PGM in CLHP reactions.

Kataria, Yeo [47] simulated the profiles for a multi-tubular reducer with isothermal operation, where the temperature control was achieved through a heating/cooling fluid supply on the shell side. The reactions were demonstrated in the tubes with the assumption of negligible radial profiles due a large length-diameter ratio (L_t/D_t > 50). Further assumptions were defined through PGM, involving the diffusion of gas into the porous pellet. The diffused fluid reacts through the surface of microscopic grains, which were considered nonporous due to negligibility at the pellet scale. Profiles from a single pellet were compiled a over a small tube section, and the output flows were then utilized to initialize the next differential length. The iterations were repeated with the addition of each section, resulting in the profiles representing complete reactor length. The MBR vessel was assumed to operate in countercurrent flow, where the solids flow downward from top and the gas flows upwards from the bottom. A schematic illustration of the model is represented in Figure 2, describing the multi-scale process.

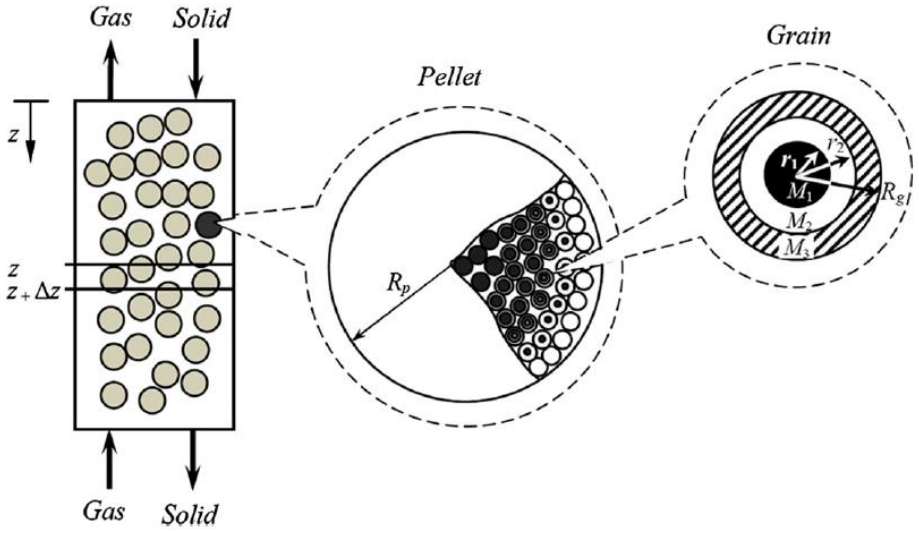

Figure 2. Illustration of the proposed gas-solid system in a counter-current MBR tube [34].

The Fe_2O_3 pellet reacting within the reducer undergoes consecutive reduction, resulting in presence of multiple solid phases. The terms M1 (Fe_2O_3), M2 (Fe_3O_4), and M3 (FeO) were assigned to the oxidation states of the OC based on their sequence of generation. In addition to stagewise solid phase change, parallel reactions from both syngas species CO and H_2 (referred as A and C in equations) were also considered. The conversion of solids was modelled as a function of gas reaction rates (*Rj*), which is a function of the respective concentration diffused into the pellet ($C_{t,p}$) and reaction temperature (T). The reaction kinetic data were retrieved from Negri, Alfano [48], and may be utilized to reproduce the current simulation. Changes within the innermost solid surface M1 were described through its radius r_1 and the surface reactions from both gases with respect to time (t), as shown in (1).

$$\frac{dr_1}{dt} = -\frac{1}{\rho_1}\left[\alpha_{A(I)}R_{A(I)} + \alpha_{C(I)}R_{C(I)}\right] = -\frac{1}{\rho_1}\sum_{j=A,C}\alpha_j R_j \qquad (1)$$

The terms α and ρ refer to the gas stoichiometric coefficient and solid phase density, respectively. Solid phase M2 is consecutively produced by the first reaction and consumed through the second during reactions. The effective volume of M2 present in the grain is calculated through the remaining volume from the reduced core ($\frac{4}{3}\pi({r_2}^3 - {r_1}^3)$). Utilizing a similar derivative approach, molar profiles of each reactant phase M_i with $i > 1$ can be calculated through (2).

$$\frac{dr_i}{dt} = -\frac{1}{\rho_i}\sum_{j=A,C}\alpha_j R_j + \frac{r_{i-1}^2}{r_i^2}\left\{\frac{1}{\rho_i}\sum_{j=A,C}\beta_{j(i-1)}R_{j(i-1)} - \sum_{j=A,C,\cdots}^{m_i} - \frac{1}{\rho_{i-1}}\sum_{j=A,C}\alpha_{j(i-1)}R_{j(i-1)}\right\} \qquad (2)$$

The term β indicates the solid phase stoichiometric coefficient, during reaction with a given gas species (j). Gas diffusion into the pellet was assumed as Knudsen type, allowing estimation of the inlet flow through the pellet surface. The concentration difference between the bulk ($C_{t,b}$) and pellet phases ($C_{t,p}$) were utilized to estimate the diffusive flux Nj, and its relevant correlation can be referred from Yang, Gu [49]. Although the inward radial flow of gases can develop concentration profiles within the granular pellet, the changes were assumed to be negligible on a reactor scale. The even distribution of diffused gas allowed integration of grain conversion over the entire pellet structure. The material balance for gas species at the pellet scale was then established through the inward diffusion and conversion to product through reactions, as shown in (3).

$$\frac{\partial(\varepsilon_p C_{t,p} y_{j,p})}{\partial t} = \frac{N_j . A_p}{V_p} - \frac{3(1-\varepsilon_p)}{R_g^3}\sum_{i=1,2,3}\sum_{j=A,C} r_i^2 R_j \qquad (3)$$

The terms ε_p, A_p, and V_p refer to the porosity, surface area and volume of the pellet, respectively. The parameter R_g indicates grain radius, and $y_{j,p}$ demonstrates the gas mole fraction inside the pellet. The pellet behaviour can be readily scaled up over the reactor due to the previous defined MBR assumption of uniform radial profiles. Gas generates concentration profiles along the axial reactor length (z), which are computed in the bulk phase according to (4).

$$\frac{\partial}{\partial z}\left(u_g\, c_{t.b}\, y_{j,b}\right) = -\left[\frac{A_p \dot{n}_p}{A_b u_s}\left(N_j - \sum_{j=1}^{k} R_j\right)\right] \qquad (4)$$

The terms u_g and $y_{j,b}$ refer to the velocity and bulk mole fraction of a given gas species, whereas A_b and u_s indicate the solid bed surface area and velocity. The parameter $\dot{n}_p$ describes the number of pellets entering the system per unit time, which can be estimated using the pellet volume flow and available bed length. The correlation presented in (4) models the bulk phase interactions in a stationary fixed-bed reactor, which is valid assuming that the solid flow is negligible compared to the gas ($u_g \gg u_s$). The equations mentioned above provide a brief description of the modelling procedures required to develop the proposed reducer simulation, and the methods can be repeated for expressing oxidizer and combustor systems. The detailed derivations and modelling procedures are available through the literature cited and can be referred for further information [34, 47]. The initialization parameters are described in Table 1, which were utilized to generate the initial reducer profiles.

Table 1. Initial specifications for the reducer

Parameter (units)	Value
D_t (cm)	25
R_p (cm)	0.61
ε_p	0.22
Gas flow (cm^3/s)	28,666.67
Solid flow (g/s)	17.39
Mole ratio H_2/CO	2
T (K)	1,173
Pressure (atm)	20

3. Results and Discussion

3.1. Previous findings

Prior to presenting the results, it is necessary to establish the background of previous investigations conducted within this research project. Kataria, Yeo [47] simulated the isothermal reducer profiles based on the parameters from Table 1. Findings revealed that the solid conversion was restricted to the FeO phase, which can be utilized within the oxidizer for H2 production. The profiles also indicated that the H_2 from the reactant gas was completely removed, whereas large amounts of CO (~ 32.9 mol %) remained unconverted. The observed deviations were justified through the selected operating conditions and equilibrium phase diagrams. The system was further subjected to modification in the reactant flow rates using the gas-solid ratio (V_{gs}), where no noticeable impact was observed with considerable reduction. A significant impact was observed around 682 ($cm^{-3}.s^{-1}$ gas/ $cm^{-3}.s^{-1}$ solid), and lower values accelerated the conversion. The tests were stopped at a value of 170, which indicated a minimum flow rate ratio (Solid flow = 1% of the gas) to approximate the MBR profiles as a fixed bed. The examination concluded with the unconverted CO gas (~ 27.5 mol %), suggesting further optimization using additional considerations such as bed porosity and reaction temperature. Recommendations from the National Physical Laboratory indicate a minimum gas purity of 95% for employing a successful CCS strategy through conceptual designs [50]. The current analysis serves as an extension of the study conducted by Kataria, Yeo [47],

where the model is subjected to further modifications using recommended parameters. The investigation is aimed at achieving conversions within the desired purity limits (< 5%), along with additional modelling procedures to study the oxidizer system.

3.2. Reducer optimization

The simulated reduction process assumes reactions within spherical pellets of uniform diameter (D_p), in a counter current MBR with no radial profiles (due to tubular design) [51]. Porosity of the packed bed (ε_b) is an essential parameter, due to its impact on the effective solid surface available for gas diffusion and reaction. The correlation for ε_b was utilized within the dynamic model and can be referred from the previous investigation [47]. The equation depicts an inverse relationship with the tube-to-pellet diameter ratio (D_t/D_p), suggesting that these parameters may present an impact on CO conversion. The system was subjected to modification of D_t, in accordance with several standard sizes from the American Society of Mechanical Engineers (ASME). Values of D_p were also consecutively reduced to lower voidage, and the test was conducted over four industry-grade sizes [52]. Figure 3 illustrates the impact of bed porosity on CO mole fraction, highlighting effectiveness of the selected variables.

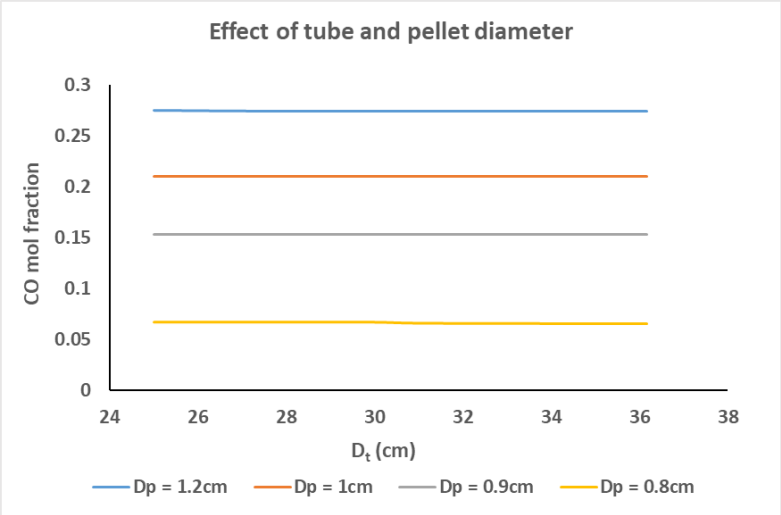

Figure 3. Impact of reducer bed porosity on CO conversion

Results indicate a negligible influence over a wide range of D_t values, whereas D_p exhibited considerable effects. Reduction of the pellet size improved the outlet CO mol fraction by a significant margin, and the lowest available size (0.8 cm) produced only 6.5 mol % in the outlet stream. The optimization tests did not depict any noticeable changes in the H_2 and solid performances, and thus their profiles are not displayed. These findings confirm the hypothesis surrounding the impact of bed porosity on isothermal reducer efficiency, representing a vital contribution to the CLHP literature. Another advantage of reducing the pellet size is the enhancement of mechanical strength, consequently promoting resistance to abrasion and sintering [53]. The reactor system is solved through an iterative technique, compiling the axial profiles generated within multiple smaller sections. The model can be scaled up by addition of length representing the solid volume, along with consecutive elevation in the gas flow to maintain the V_{gs} value and pellet residence time (gas contact time). However, u_g must be kept below the fluidization regime (u_{mf}) to ensure moving bed operation [54]. Thus, the gas velocity limitation describes a maximum allowable reactor length. On the other hand, the length-diameter constraint for the tube ($L_t/ D_t > 50$) represents another essential restriction necessary to avoid radial profiles within the tubular vessel [51]. Thus, it is imperative to identify scale-up limits based on the selected pellet size prior to attempting a commercial design. The value of u_{mf} (~ 6.12 $m.s^{-1}$) was determined using the correlations within literature, employing the D_p recommended using the results from Figure 3. Additionally, the minimum required length (~ 13.2 m) was estimated by using D_t as the nearest standard ASME size (26.4

cm). Gas flow at the specified length (~ 1.67 $m^3.s^{-1}$) produced velocities well below the u_{mf} range (u_g ~ 2.54 m/s), suggesting that the process conditions are safe for industrial-scale applications. Moreover, the considerably lower u_g value also presents potential for further increments in length without violating the flow constraint. A detailed design of the large-scale system is not included within the scope of current study and presents scope for further investigations. The presented findings may prove essential for future research, aimed at evaluating commercial limitations of the CLHP process.

Evaluation of the changes in the pellet and tube sizes remained insufficient in achieving the purity targets (> 95% syngas conversion) necessary for implementing an effective CCS strategy. The system was then subjected to temperature modifications, representing a crucial model parameter controlled through a heating/cooling fluid supplied in the shell of the reactor vessel. Figure 4 displays the concentrations (mol %) of H_2 and CO in response to the applied changes, where the solid performance was not shown due to negligible effects.

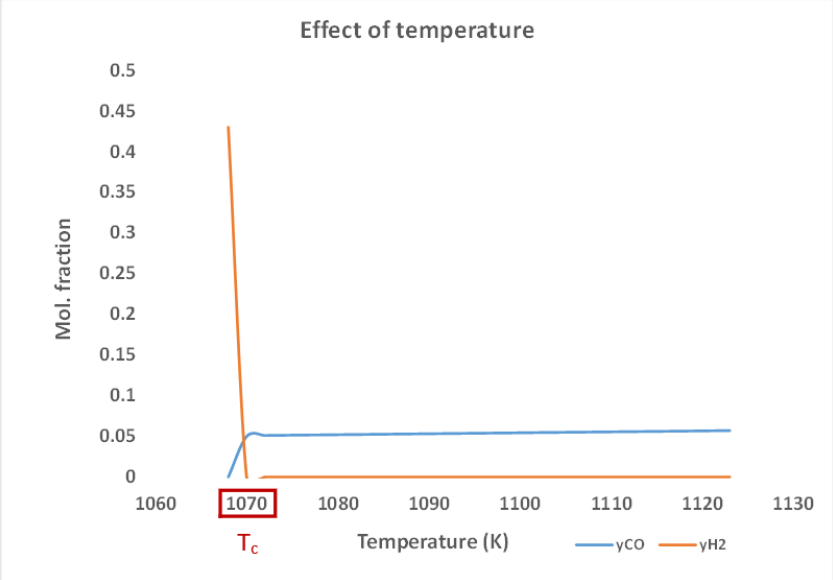

Figure 4. Effects of temperature on syngas conversion in the reducer

Results in Figure 4 suggest a minimal impact on the CO concentration with up to 100 K (1173K – 1073) reduction, and a critical temperature (T_c ~ 1070 K) was identified below which complete conversion was achieved. However, values lower than T_c resulted in large amounts unconverted H_2 present within the outlet stream. These findings describe a trade-off point between the reaction dynamics of syngas components, which can be utilized for developing a control strategy to achieve optimum performance. In the reaction profiles demonstrated by Kataria, Yeo [47], the H_2 was primarily converted at the bottom of the bed through the reactions involving production of Fe from FeO. The Fe_2O_3 and Fe_3O_4 states were reduced through CO at the top, indicating that an allowable temperature drop (ΔT) may be beneficial for the process kinetics. Lower sections of the reactor require a higher heat supply to maintain temperature higher than the critical point ($T_{bottom} > T_c$) for promoting H_2 reactions, and the ΔT must be ensured over the effective tube length for complete CO conversion. Based on the current findings, a 10 K temperature drop is sufficient to completely consume the reactant gas. The proposed range can be further investigated within future investigations focusing on control system analysis, representing additional prospects arising from this study. Moreover, the CO fraction observed at T_c (~ 4.92 mol %) is within the desired purity constraints, suggesting that CCS can be successfully implemented using the presented reducer design. Therefore, the optimum operating conditions of the isothermal CLHP reducer can be utilized for achieving the desired gas-solid production targets.

3.3. Oxidizer simulation

The simulation model was further extended by incorporating the oxidizer design, utilizing similar PGM-based dynamics from the reduction process. The pellet outflow, solid concentration and reaction temperature exiting the reducer were employed as the initial conditions. The V_{gs} was also maintained at the previous value, allowing computation of the required inlet steam flow rate. Furthermore, the tube dimensions (D_t and L_t) were also taken identical to the previous unit, which conserved the overall gas-solid contact time within the vessel. Majority of the input parameters were conserved to simulate inter-connected reactors, where the product from reducer can be directly fed to the oxidizer without any preprocessing. The reaction kinetic data (Reaction rate and equilibrium constant) were modelled as reverse reactions of the H_2-based reduction process, defined previously within the reducer. Reaction profiles for the oxidizer MBR were generated as both co-current and counter-current flows for comparison, as exhibited in Figure 5.

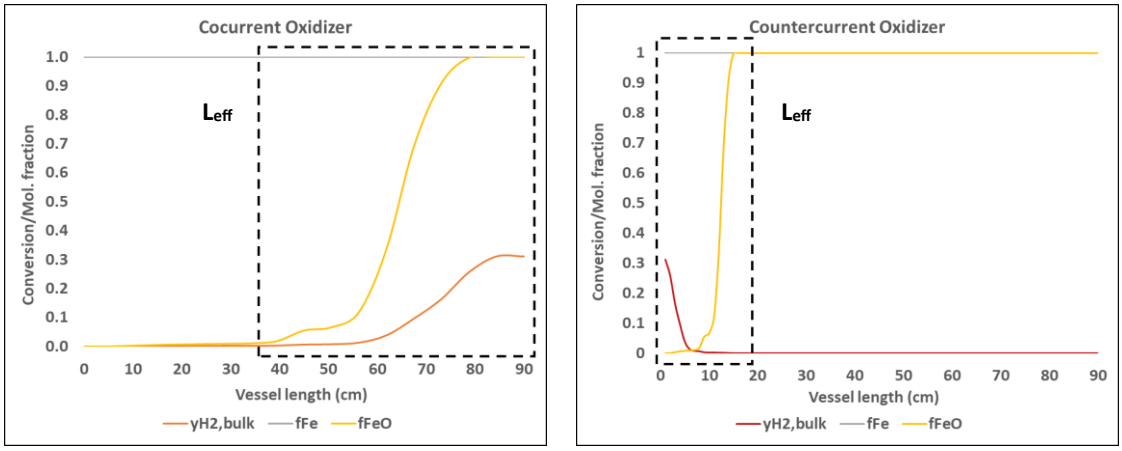

(**a**) (**b**)

Figure 5. Isothermal oxidizer profiles representing (a) Co-current and (b) Counter-current flow.

The simulated reactions in Figure 4 indicate that both flows achieved identical conversions, with the solid completely oxidized to the desired state (Fe_3O_4) and around 30 mol % H_2 in the outlet gas. Despite similar outcomes, the effective length of the reaction zone (L_{eff}) differs significantly between the two configurations. The counter-current strategy presented a smaller value of L_{eff} (~ 20 cm), which is likely due to the improved gas-solid contact time of the flow regime [55]. Exothermicity of the oxidizer reactions is a vital consideration for implementing a temperature control system with effective heat removal, which may be inefficient over shorter lengths. The sharp increase in system heat may lead to a significant deviation, consequently impacting other process parameters. Thus, co-current approach proves beneficial in the oxidizer case as it displays a significant improvement in the reaction zone size (L_{eff} ~ 50 cm). These findings describe crucial implications regarding commercial reactor design procedures for CLHP, which may be attempted in future investigations.

3.4. Oxidizer optimization

Optimization for the steam oxidation process presents further challenges, due to several constraints arising from the interconnected reactor system. The pellet movement is constrained by the reducer outlet, which consequently restricts the reduction of gas flow through the minimum V_{gs} (~ 170) required for maintaining MBR dynamics. The H_2 conversions are analyzed as a function of the reaction temperature, which was highlighted as a critical parameter in implementing the CCS. The observations are displayed in Figure 6, representing the effects of temperature on the product mole fraction.

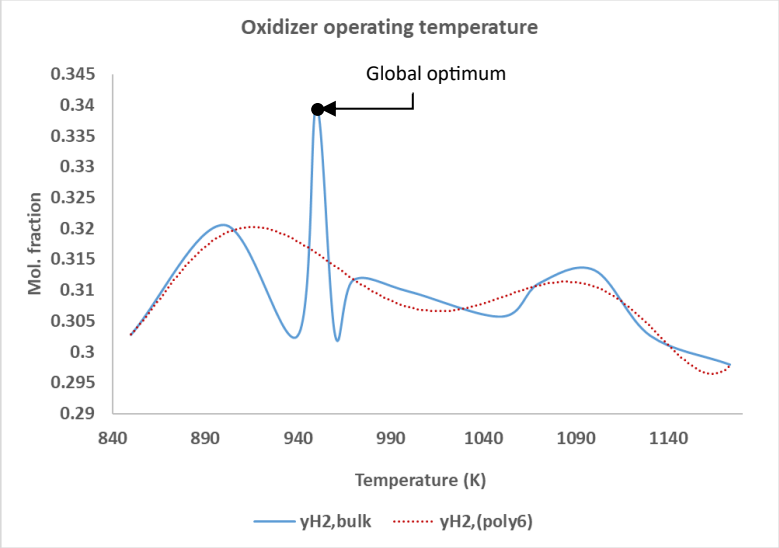

Figure 4. Effects of temperature on syngas conversion in the reducer

The outlet gas concentration (yH_2, bulk) from the oxidizer presents substantial deviations through temperature changes, leading to function with several optima. Such non-linear behavior may arise due to comparable diffusion-reaction rates within the process, promoting variability within the output concentrations [56]. Operating in a reaction-dominated regime is recommended to avoid the instability, although it might impose limitations on industrial applications. A large temperature difference from the reducer values may lead to degradation of the pellet, causing loss of essential mechanical properties [57]. Damage to the solid surface may require frequent replacements, thus lowering the efficiency of continuous production. Hence, the current range is considered suitable for avoiding significant heat changes and maintaining the longevity of OC circulation. The global optimum was identified at 950 K, producing 34 mol % H_2 in the outlet stream. However, the optimum is achieved within a narrow range (± 5K) and may produce challenges in implementing a capable controller.

The issue of overcomplexity can be resolved using polynomial approximations, allowing identification of patterns or directions within a dynamic response [58]. A sixth-order trend (yH_2, (poly6)) was projected over the trends in Figure 5, which describe a moving average of the H_2 temperature-conversion function. The updated dynamics clearly indicate improvements through temperature reduction, although the variations are substantial at lower temperatures. From a control system perspective, achieving higher conversion for H_2 may a challenging task. Higher range (1000 – 1100 K) is recommended to restrict sudden changes due to minor temperature deviation, potentially resulting in a reduced cost and computation for controller design. Lower temperatures may be employed for boosting process productivity, though the deployed control system must be capable of limiting the deviations within a range (950 ± 5K). Thus, industrial application of the CLHP oxidizer requires strategic decision-making from the engineers based on available technology and resources. The results from this study are tabulated in Table 2, indicating the difference between optimum and initial values of the evaluated parameters.

Table 2. Initial and optimum values of the evaluated parameters.

Parameter	Initial	Recommended optimum
D_p	1.22 cm	0.8 cm
D_t	25 cm	26.4 cm
T (reducer)	1173 K	1070 K
T (oxidizer)	1070 K	950 K

Further process optimization necessitates modification of the solid flow from reducer, which may result in a re-iteration of the devised operating conditions. The inherent dependence of inter-connected units is apparent through the restrictions imposed on the current oxidizer, and the combustor model may provide further information regarding the complete characteristics of the closed-loop CLHP process. The overall aim of this simulation and optimization analysis is to determine the maximum achievable process efficiency under realistic conditions, which can provide a basis for designing the industrial reactors. Commercial implementation of technologies such as CLHP is vital to ensure sustainable energy production at a large scale, which is necessary to tackle the consistently rising issue of global warming.

4. Conclusions

Dynamic behavior of the CLHP reducer and oxidizer were analyzed in this study, aimed at optimizing performance for continuous production. The reactors were simulated as inter-connected tubular MBRs, which can maintain isothermal operation and circulate the solid OC. Reaction kinetics were described using PGM for achieving high accuracy estimates of gas-solid reactions, based on the modelling procedures conducted by Kataria, Yeo [47] for the reducer. The gas-solid ratio (V_{gs}) was previously reported to present limited impact, which resulted in large amount of unconverted CO (~ 27.5 mol %) in the outlet stream. The process was further enhanced in the current investigation by employing changes in pellet dimensions and reaction temperature, thereby reducing the impurity to a specified limit (< 5%) for achieving an efficient CCS design. Pellet size reduction caused a drop in the u_{mf} values, which can restrict gas flow on a larger scale. However, the presented reducer could achieve the minimum required length (~ 13.2 m) to avoid radial profiles as the u_{mf} limit (~ 6.12 m/s) was not exceeded by the computed gas velocity (~ 2.54 m/s).

Final reducer outflows were then utilized to develop the oxidizer simulation, which was analyzed under co-current and counter current MBR flow regimes. The findings indicated a narrow reaction zone for the counter-current strategy, which may limit heat exchange necessary to achieve isothermal operations. The co-current method was thus recommended for achieving stable H_2 concentrations under a large-scale design. The inter-connectivity of the reactors imposed several parametric constraints on the oxidizer, allowing optimization of the system solely through temperature. The applied modifications displayed significant variations within the conversion, with a 5 mol % improvement in the output concentration at the identified global optimum (950 K). However, the proposed enhancement was applicable within a narrow range (± 5 K) along with large deviations at the surrounding values. Hence, operating within lower temperatures may result in an expensive controller design and requires a cost-benefit analysis prior to devising an optimum. It was recommended to operate at the higher temperature range (1000 – 1100 K) due to lower variations, which can allow engineers to develop cost-effective control systems despite some loss in the conversion. Further optimization for the oxidizer necessitates re-evaluation of the reducer operation due to inter-connectivity, which highlights the importance of conducting the current research. Combustor simulation is a crucial next step for investigating characteristics of the closed-loop process, allowing determination of the achievable optimum production under realistic constraints. The optimized dynamic model can then be implemented in the development of an adequate control system and scale-up design, serving as the ultimate aim of the proposed research.

Acknowledgments: The authors would like to thank the organizers of Process Control Virtual Symposium (PCVS) for providing a platform to present the findings of this research. The authors would also like to thank Curtin University Malaysia for their consistent support throughout the project.

References

1. Pasten C, Santamarina JC. Energy and quality of life. Energy Policy. 2012/10/01/ 2012;49:468-476. doi:https://doi.org/10.1016/j.enpol.2012.06.051
2. Energy use (kg of oil equivalent per capita) - Malaysia. Accessed November 2023. https://data.worldbank.org/indicator/EG.USE.PCAP.KG.OE?end=2014&locations=MY&start=1971&view=chart
3. Fossil fuel energy consumption (% of total) - Malaysia. Accessed November 2023. https://data.worldbank.org/indicator/EG.USE.COMM.FO.ZS?end=2014&locations=MY&start=1971&view=chart
4. Combustible renewables and waste (% of total energy) - Malaysia. Accessed November 2023. https://data.worldbank.org/indicator/EG.USE.CRNW.ZS?end=2014&locations=MY&start=1971&view=chart
5. Wang B, Wang Z. Heterogeneity evaluation of China's provincial energy technology based on large-scale technical text data mining. Journal of Cleaner Production. 2018;202:946-958.
6. Ritchie H, Roser M, Rosado P. CO_2 and Greenhouse Gas Emissions. Our World in Data. 2020;
7. Qazi A, Hussain F, Rahim NA, et al. Towards Sustainable Energy: A Systematic Review of Renewable Energy Sources, Technologies, and Public Opinions. IEEE Access. 2019;7:63837-63851. doi:10.1109/ACCESS.2019.2906402
8. Tanzer SE, Blok K, Ramírez A. Can bioenergy with carbon capture and storage result in carbon negative steel? International Journal of Greenhouse Gas Control. 2020/09/01/ 2020;100:103104. doi:https://doi.org/10.1016/j.ijggc.2020.103104
9. Zohuri B. Nuclear fuel cycle and decommissioning. Nuclear Reactor Technology Development and Utilization. Elsevier; 2020:61-120.
10. Kurniawan TA, Othman MHD, Singh D, et al. Technological solutions for long-term storage of partially used nuclear waste: A critical review. Annals of Nuclear Energy. 2022;166:108736.
11. Crabtree GW, Dresselhaus MS. The Hydrogen Fuel Alternative. MRS Bulletin. 2008;33(4):421-428. doi:10.1557/mrs2008.84
12. Cao L, Yu IKM, Xiong X, et al. Biorenewable hydrogen production through biomass gasification: A review and future prospects. Environmental Research. 2020/07/01/ 2020;186:109547. doi:https://doi.org/10.1016/j.envres.2020.109547
13. Seyitoglu SS, Dincer I, Kilicarslan A. Energy and exergy analyses of hydrogen production by coal gasification. International Journal of Hydrogen Energy. 2017/01/26/ 2017;42(4):2592-2600. doi:https://doi.org/10.1016/j.ijhydene.2016.08.228
14. Holappa L. A General Vision for Reduction of Energy Consumption and CO2 Emissions from the Steel Industry. 2020;10(9):1117.
15. Wilberforce T, Olabi AG, Sayed ET, Elsaid K, Abdelkareem MA. Progress in carbon capture technologies. Science of The Total Environment. 2021/03/20/ 2021;761:143203. doi:https://doi.org/10.1016/j.scitotenv.2020.143203
16. Norskov JK, Christensen CH. Toward Efficient Hydrogen Production at Surfaces. 2006;312(5778):1322-1323. doi:doi:10.1126/science.1127180
17. Gielen D, Simbolotti G. Prospects for hydrogen and fuel cells. International Energy Agency Paris; 2005.
18. Khan MN, Shamim T. Techno-economic assessment of a plant based on a three reactor chemical looping reforming system. International Journal of Hydrogen Energy. 2016/12/28/ 2016;41(48):22677-22688. doi:https://doi.org/10.1016/j.ijhydene.2016.09.016
19. Shaner MR, Atwater HA, Lewis NS, McFarland EW. A comparative technoeconomic analysis of renewable hydrogen production using solar energy. 10.1039/C5EE02573G. Energy & Environmental Science. 2016;9(7):2354-2371. doi:10.1039/C5EE02573G
20. Huya-Kouadio J. Doe hydrogen and fuel cells program record. 2017;

21. Lim Z-W, Goh K-L. Natural gas industry transformation in Peninsular Malaysia: The journey towards a liberalised market. Energy Policy. 2019;128:197-211.
22. Mainali B, Pachauri S, Rao ND, Silveira S. Assessing rural energy sustainability in developing countries. Energy for Sustainable Development. 2014/04/01/ 2014;19:15-28. doi:https://doi.org/10.1016/j.esd.2014.01.008
23. Singh R, Wang X, Mendoza JC, Ackom EK. Electricity (in)accessibility to the urban poor in developing countries. WIREs Energy and Environment. 2015;4(4):339-353. doi:https://doi.org/10.1002/wene.148
24. Winkler H, Simões AF, Rovere ELl, Alam M, Rahman A, Mwakasonda S. Access and Affordability of Electricity in Developing Countries. World Development. 2011/06/01/ 2011;39(6):1037-1050. doi:https://doi.org/10.1016/j.worlddev.2010.02.021
25. Kolster C, Mechleri E, Krevor S, Mac Dowell N. The role of CO2 purification and transport networks in carbon capture and storage cost reduction. International Journal of Greenhouse Gas Control. 2017/03/01/ 2017;58:127-141. doi:https://doi.org/10.1016/j.ijggc.2017.01.014
26. Dickinson NL. Treatment of solid carbon containing materials to produce carbon monoxide for the synthesis of organic materials. Google Patents; 1952.
27. Jones MC. Production of mixtures of carbon monoxide and hydrogen. Google Patents; 1953.
28. Lewis WK, Gilliland ER. Production of pure carbon dioxide. Google Patents; 1954.
29. Chen L, Qi Z, Zhang S, Su J, Somorjai G. Catalytic Hydrogen Production from Methane: A Review on Recent Progress and Prospect. Catalysts. 08/02 2020;10:858. doi:10.3390/catal10080858
30. Chiesa P, Lozza G, Malandrino A, Romano M, Piccolo V. Three-reactors chemical looping process for hydrogen production. International Journal of Hydrogen Energy. 2008/05/01/ 2008;33(9):2233-2245. doi:https://doi.org/10.1016/j.ijhydene.2008.02.032
31. Long Y, Gu Z, Lin S, et al. NiO and CuO coated monolithic oxygen carriers for chemical looping combustion of methane. Journal of the Energy Institute. 2021/02/01/ 2021;94:199-209. doi:https://doi.org/10.1016/j.joei.2020.09.004
32. Mirzajani A, Ebrahim H, Nouri S. Simulation of a direct reduction moving bed reactor using a three interface model. Brazilian Journal of Chemical Engineering. 2018;35:1019-1028.
33. Zhou Q, Zeng L, Fan L-S. Syngas Chemical Looping Process: Dynamic Modeling of a Moving-Bed Reducer. Research Gate. 2013. Accessed August 5. https://www.researchgate.net/publication/256112858_Syngas_chemical_looping_process_Dynamic_modeling_of_a_moving-bed_reducer
34. Rahimi A, Niksiar A. A general model for moving-bed reactors with multiple chemical reactions part I: Model formulation. International Journal of Mineral Processing. 2013;124:58-66.
35. Monazam ER, Breault RW, Siriwardane R. Kinetics of Magnetite (Fe3O4) Oxidation to Hematite (Fe2O3) in Air for Chemical Looping Combustion. Industrial & Engineering Chemistry Research. 2014:13320-13328.
36. Tong A, Sridhar D, Sun Z, et al. Continuous high purity hydrogen generation from a syngas chemical looping 25kWth sub-pilot unit with 100% carbon capture. Fuel. 2013/01/01/ 2013;103:495-505. doi:https://doi.org/10.1016/j.fuel.2012.06.088
37. Zhu J, Araya SS, Cui X, Sahlin SL, Kær SK. Modeling and Design of a Multi-Tubular Packed-Bed Reactor for Methanol Steam Reforming over a Cu/ZnO/Al2O3 Catalyst. 2020;13(3):610.
38. Oyegoke T, Adamu Y, Fasanya O, et al. Design and Fabrication of a Multi-tubular Fixed Bed Reactor for Acetone Production as A Pilot Plant Model for Chemical Engineering Training in Developing Nations. Journal of the Pakistan Institute of Chemical Engineers. 2022;50(2)
39. Kang K-S, Kim C-H, Bae K-K, Cho W-C, Kim S-H, Park C-S. Oxygen-carrier selection and thermal analysis of the chemical-looping process for hydrogen production. International Journal of Hydrogen Energy. 2010/11/01/ 2010;35(22):12246-12254. doi:https://doi.org/10.1016/j.ijhydene.2010.08.043
40. Kataria P, Nandong J, Yeo WS. Reactor design and control aspects for Chemical Looping Hydrogen Production: A review. IEEE; 2022:208-214.

41. Zhang X, Jin H. Thermodynamic analysis of chemical-looping hydrogen generation. Applied Energy. 2013/12/01/ 2013;112:800-807. doi:https://doi.org/10.1016/j.apenergy.2013.02.058
42. Szekely J. Gas-solid reactions. Elsevier; 2012.
43. Siddiqui H, Gupta A, Mahajani SM. Non-equimolar transient grain model for CO2-gasification of single biomass char pellet. Fuel. 2021/06/01/ 2021;293:120389. doi:https://doi.org/10.1016/j.fuel.2021.120389
44. Lu L, Morris A, Li T, Benyahia S. Extension of a coarse grained particle method to simulate heat transfer in fluidized beds. International Journal of Heat and Mass Transfer. 2017/08/01/ 2017;111:723-735. doi:https://doi.org/10.1016/j.ijheatmasstransfer.2017.04.040
45. Liu M, Kang Q, Xu H. Grain-scale study of the grain boundary effect on UO2 fuel oxidation and fission gas release under reactor conditions. Chemical Engineering Science. 2021/01/16/ 2021;229:116026. doi:https://doi.org/10.1016/j.ces.2020.116026
46. Takenaka Y, Kimura Y, Narita K, Kaneko D. Mathematical model of direct reduction shaft furnace and its application to actual operations of a model plant. Computers & chemical engineering. 1986;10(1):67-75.
47. Kataria P, Yeo WS, Nandong J. Dynamic model of isothermal moving bed reducer for chemical looping hydrogen production. EDP Sciences; 2023:01017.
48. Negri ED, Alfano OM, Chiovetta MG. Moving-bed reactor model for the direct reduction of hematite. Parametric study. Industrial & engineering chemistry research. 1995;34(12):4266-4276.
49. Yang F, Gu J, Ye L, et al. Justifying the significance of Knudsen diffusion in solid oxide fuel cells. Energy. 2016/01/15/ 2016;95:242-246. doi:https://doi.org/10.1016/j.energy.2015.12.022
50. Murugan A, Gardiner T, Brown RJ, et al. Purity requirements of carbon dioxide for carbon capture and storage. 2019;
51. Zhu J, Araya SS, Cui X, Sahlin SL, Kær SK. Modeling and design of a multi-tubular packed-bed reactor for methanol steam reforming over a Cu/ZnO/Al2O3 catalyst. Energies. 2020;13(3):610.
52. Dwarapudi S, Devi TU, Rao SM, Ranjan M. Influence of pellet size on quality and microstructure of iron ore pellets. ISIJ international. 2008;48(6):768-776.
53. Umadevi T, Kumar P, Lobo NF, Mahapatra PC, Prabhu M, Ranjan M. Effect of Iron Ore Pellet Size on its Properties and Microstructure. steel research international. 2009;80(10):709-716. doi:https://doi.org/10.2374/SRI08SP169
54. Cocco R, Karri SR, Knowlton T. Introduction to fluidization. Chem Eng Prog. 2014;110(11):21-29.
55. Okoli CO, Ostace A, Nadgouda S, et al. A framework for the optimization of chemical looping combustion processes. Powder Technology. 2020/04/01/ 2020;365:149-162. doi:https://doi.org/10.1016/j.powtec.2019.04.035
56. Niksiar A, Rahimi A. A study on deviation of noncatalytic gas–solid reaction models due to heat effects and changing of solid structure. Powder Technology. 2009/07/10/ 2009;193(1):101-109. doi:https://doi.org/10.1016/j.powtec.2009.02.012
57. Baniasadi M, Peters B, Pierret J-C, Vanderheyden B, Ansseau O. Experimental and numerical investigation into the softening Behavior of a packed bed of iron ore pellets. Powder Technology. 2018/11/01/ 2018;339:863-871. doi:https://doi.org/10.1016/j.powtec.2018.08.035
58. Hodyss D. Ensemble State Estimation for Nonlinear Systems Using Polynomial Expansions in the Innovation. Monthly Weather Review. 01 Nov. 2011 2011;139(11):3571-3588. doi:10.1175/2011mwr3558.1